Control Engineering Practice 20 (2012) 148–155

Contents lists available at SciVerse ScienceDirect

Control Engineering Practice

journal homepage: www.elsevier.com/locate/conengprac

Globally exponentially stable cascade observers for attitude estimation ☆

Pedro Batista [a,*], Carlos Silvestre [a,b], Paulo Oliveira [a]

[a] Institute for Systems and Robotics, Instituto Superior Técnico, Universidade Técnica de Lisboa, Av. Rovisco Pais, 1049-001 Lisboa, Portugal
[b] Faculty of Science and Technology, University of Macau, Taipa, Macau

ARTICLE INFO

Article history:
Received 4 April 2011
Accepted 3 October 2011
Available online 9 November 2011

Keywords:
Attitude algorithms
Observers
Observability
Estimation
Navigation systems

ABSTRACT

This paper presents the design, analysis, and performance evaluation of a novel cascade observer for attitude estimation. A sensor-based observer, which resorts to rate gyro readings and a set of vector observations, estimates the rate gyro bias. Afterwards, a cascaded observer explicitly estimates the attitude in the form of a rotation matrix based on the rate gyro measurements, the vector observations, and the estimated gyro bias. The overall error dynamics are globally exponentially stable and the proposed system is computationally efficient. Finally, the resulting estimator is successfully evaluated, in simulation and experimentally, with ground truth data in both cases.

1. Introduction

Attitude estimation has been a hot topic of research in the recent years, as evidenced by the large number of publications on the subject, see e.g. Metni, Pflimlin, Hamel, and Soueres (2006), Tayebi, McGilvray, Roberts, and Moallem (2007), Campolo, Keller, and Guglielmelli (2006), and Choukroun (2009). The Extended Kalman Filter (EKF) has been at the core of numerous stochastic solution, see e.g. Farrell (1970), Bar-Itzhack and Oshman (1985), and Sabatini (2006), while nonlinear alternatives, aiming for stability and convergence properties, have been proposed in Sanyal, Lee, Leok, and McClamroch (2008), Vasconcelos, Cunha, Silvestre, and Oliveira (2007), Rehbinder and Ghosh (2003), Mahony, Hamel, and Pflimlin (2008), Thienel and Sanner (2003), and Martin and Salaun (2010), to mention just a few, see Crassidis, Markley, and Cheng (2007) for a thorough survey on the subject of attitude estimation.

Lack of convergence guarantees, singularities, unwinding phenomena, topological limitations for achieving global asymptotic stability, and slow convergence near unstable equilibrium points are common drawbacks of attitude estimation solutions, see Bhat and Bernstein (2000) and Chaturvedi, Sanyal, and McClamroch (2011). In previous work by the authors, Batista, Silvestre, and Oliveira (2009), a sensor-based attitude estimation filter was derived that has globally asymptotically stable (GAS) error dynamics and does not carry any of the aforementioned limitations. Unfortunately, that solution is computational expensive. Indeed, it requires the solution of a matrix differential Riccati equation associated to a state of dimension $3N$, where N is the number of vector observations. In addition, the final rotation matrix is obtained from the solution of the Wahba's problem, which involves, in general, a singular value decomposition (SVD) problem.

The main contribution of this paper is the design, analysis, and performance evaluation of a novel cascade attitude observer that: (i) has globally exponentially stable (GES) error dynamics; (ii) is computationally efficient; (iii) is based on the angular motion kinematics, which are exact, in contrast with dynamic models, which usually contain uncertain and unmodeled dynamics; (iv) builds on well-established Lyapunov results; (v) explicitly estimates rate gyro bias and copes well with slowly time-varying bias; and (vi) has a complementary structure, fusing low bandwidth vector observations with high bandwidth rate gyro measurements. In this paper, the sensor measurements are included directly in the system dynamics, following the approach introduced in Batista et al. (2009), and the kinematics are propagated using the angular velocity provided by a three-axis rate gyro, whose bias is also considered. A novel computationally efficient observer is designed for this system, that yields an estimate of the rate gyro bias, and that feeds a second novel observer for the rotation matrix, which is also computationally efficient. The overall closed-loop error dynamics are shown to be GES and the estimates of the rotation matrix converge asymptotically to the Special Orthogonal Group, $SO(3)$. An additional solution refinement is provided that yields solutions arbitrarily close to $SO(3)$, keeping at the same time low computational requirements.

☆ This work was partially supported by Fundação para a Ciência e a Tecnologia (ISR/IST plurianual funding) through the PIDDAC Program funds, by the project PTDC/MAR/64546/2006—OBSERVFLY of the FCT, and by the EU Project TRIDENT (Contract No. 248497).

* Corresponding author. Tel.: +351 218418054; fax: +351 218418291.
E-mail addresses: pbatista@isr.ist.utl.pt (P. Batista), cjs@isr.ist.utl.pt (C. Silvestre), pjcro@isr.ist.utl.pt (P. Oliveira).

0967-0661/$ - see front matter © 2011 Elsevier Ltd. All rights reserved.
doi:10.1016/j.conengprac.2011.10.005

Finally, the proposed solution does not exhibit any of the aforementioned drawbacks common to attitude estimation solutions such as singularities, unwinding phenomena, slow convergence near unstable equilibrium points or topological limitations for achieving global asymptotic stabilization on $SO(3)$, see Bhat and Bernstein (2000) and Chaturvedi et al. (2011).

The paper is organized as follows. The problem statement is introduced in Section 2, whereas the observer design and stability analysis are presented in Section 3. The achieved performance is evaluated, in simulation environment, in Section 4 and experimental results are provided and discussed in Section 5. Finally, Section 6 summarizes the main contributions and conclusions of the paper.

Throughout the paper the symbol $\mathbf{0}$ denotes a matrix (or vector) of zeros and $\mathbf{I}$ an identity matrix, both of appropriate dimensions. A block diagonal matrix is represented as $\text{diag}(\mathbf{A}_1,\ldots,\mathbf{A}_n)$. For $\mathbf{x},\mathbf{y} \in \mathbb{R}^3$, $\mathbf{x}\times\mathbf{y}$ represents the cross product.

2. Problem statement

Let $\{I\}$ be an inertial reference frame, $\{B\}$ a body-fixed reference frame, and $\mathbf{R}(t) \in SO(3)$ the rotation matrix from $\{B\}$ to $\{I\}$. The attitude kinematics, expressed in the form of a rotation matrix, are given by

$$\dot{\mathbf{R}}(t) = \mathbf{R}(t)\mathbf{S}(\boldsymbol{\omega}(t)),$$

where $\boldsymbol{\omega}(t) \in \mathbb{R}^3$ is the angular velocity of $\{B\}$, expressed in $\{B\}$, and $\mathbf{S}(.)$ is the skew-symmetric matrix

$$\mathbf{S}(\boldsymbol{x}) := \begin{bmatrix} 0 & -\boldsymbol{x}_z & \boldsymbol{x}_y \\ \boldsymbol{x}_z & 0 & -\boldsymbol{x}_x \\ -\boldsymbol{x}_y & \boldsymbol{x}_x & 0 \end{bmatrix}, \quad \boldsymbol{x} = \begin{bmatrix} \boldsymbol{x}_x \\ \boldsymbol{x}_y \\ \boldsymbol{x}_z \end{bmatrix} \in \mathbb{R}^3.$$

The angular velocity is assumed to be a continuous bounded signal. Suppose that rate gyro measurements are available, corrupted by a constant bias, as given by

$$\boldsymbol{\omega}_m(t) = \boldsymbol{\omega}(t) + \mathbf{b}_\omega(t), \tag{1}$$

where $\mathbf{b}_\omega(t) \in \mathbb{R}^3$ is the rate gyro bias, which satisfies

$$\dot{\mathbf{b}}_\omega(t) = 0.$$

In addition to the rate gyro readings, suppose that a set of N vector observations $\{\mathbf{v}_i(t) \in \mathbb{R}^3, i=1,\ldots,N\}$ is available, in body-fixed coordinates, of known constant vectors in inertial coordinates

$$\mathbf{r}_i = \mathbf{R}(t)\mathbf{v}_i(t), \quad i=1,\ldots,N. \tag{2}$$

In the remainder of the paper the following assumption is made:

Assumption 1. There exist at least two non-collinear reference vectors, i.e., there exist i and j such that $\mathbf{r}_i \times \mathbf{r}_j \neq \mathbf{0}$.

This assumption is necessary for attitude estimation with constant vectors in inertial coordinates, see e.g. Mahony et al. (2008) and Batista et al. (2009), and therefore it carries no conservativeness whatsoever.

The problem considered in the paper is the design of an observer for the rotation matrix $\mathbf{R}(t)$ and the rate gyro bias $\mathbf{b}_\omega(t)$ with globally exponentially stable error dynamics.

3. Observer design and stability analysis

This section details the design of the attitude observer and the stability analysis. First, a bias observer with GES error dynamics is derived, in Section 3.1, that resorts directly to the vector observations. Afterwards, an attitude observer with GES error dynamics is proposed, in Section 3.2, assuming that the rate gyro bias is known. The overall cascade attitude observer is presented in Section 3.3, where it is shown that the resulting error dynamics are GES. Finally, refinements of the final solution are proposed and discussed in Section 3.4.

3.1. Bias observer

The set of states of the bias observer proposed in this section corresponds to the set of the vector observations, in addition to the rate gyro bias. The time derivative of the vector observations is given by

$$\dot{\mathbf{v}}_i(t) = -\mathbf{S}(\boldsymbol{\omega}(t))\mathbf{v}_i(t), \quad i=1,\ldots,N. \tag{3}$$

From (1) it is possible to rewrite (3) as

$$\begin{aligned}\dot{\mathbf{v}}_i(t) &= -\mathbf{S}(\boldsymbol{\omega}_m(t))\mathbf{v}_i(t) + \mathbf{S}(\mathbf{b}_\omega(t))\mathbf{v}_i(t) \\ &= -\mathbf{S}(\boldsymbol{\omega}_m(t))\mathbf{v}_i(t) - \mathbf{S}(\mathbf{v}_i(t))\mathbf{b}_\omega(t), \quad i=1,\ldots,N.\end{aligned}$$

Consider the bias observer given by

$$\begin{cases} \dot{\hat{\mathbf{v}}}_1(t) = -\mathbf{S}(\boldsymbol{\omega}_m(t))\hat{\mathbf{v}}_1(t) - \mathbf{S}(\mathbf{v}_1(t))\hat{\mathbf{b}}_\omega(t) + \alpha_1\tilde{\mathbf{v}}_1(t), \\ \vdots \\ \dot{\hat{\mathbf{v}}}_N(t) = -\mathbf{S}(\boldsymbol{\omega}_m(t))\hat{\mathbf{v}}_N(t) - \mathbf{S}(\mathbf{v}_N(t))\hat{\mathbf{b}}_\omega(t) + \alpha_N\tilde{\mathbf{v}}_N(t), \\ \dot{\hat{\mathbf{b}}}_\omega(t) = \sum_{i=1}^N \beta_i \mathbf{S}(\mathbf{v}_i(t))\tilde{\mathbf{v}}_i(t), \end{cases} \tag{4}$$

where $\tilde{\mathbf{v}}_i(t) := \mathbf{v}_i(t) - \hat{\mathbf{v}}_i(t)$, $i=1,\ldots,N$, are the errors of the vector observation estimates, available for stabilization purposes, and α_i,β_i, $i=1,\ldots,N$, are positive scalar constants. Define the bias estimation error as $\tilde{\mathbf{b}}_\omega(t) := \mathbf{b}_\omega(t) - \hat{\mathbf{b}}_\omega(t)$. Then, it is straightforward to show that the bias observer error dynamics are given by

$$\begin{cases} \dot{\tilde{\mathbf{v}}}_1(t) = -\mathbf{S}(\boldsymbol{\omega}_m(t))\tilde{\mathbf{v}}_1(t) - \mathbf{S}(\mathbf{v}_1(t))\tilde{\mathbf{b}}_\omega(t) - \alpha_1\tilde{\mathbf{v}}_1(t), \\ \vdots \\ \dot{\tilde{\mathbf{v}}}_N(t) = -\mathbf{S}(\boldsymbol{\omega}_m(t))\tilde{\mathbf{v}}_N(t) - \mathbf{S}(\mathbf{v}_N(t))\tilde{\mathbf{b}}_\omega(t) - \alpha_N\tilde{\mathbf{v}}_N(t), \\ \dot{\tilde{\mathbf{b}}}_\omega(t) = -\sum_{i=1}^N \beta_i \mathbf{S}(\mathbf{v}_i(t))\tilde{\mathbf{v}}_i(t), \end{cases}$$

or, in compact form

$$\dot{\tilde{\boldsymbol{x}}}_1(t) = \mathcal{A}_1(t)\tilde{\boldsymbol{x}}_1(t), \tag{5}$$

where $\tilde{\boldsymbol{x}}_1(t) = [\tilde{\mathbf{v}}_1^T(t) \ \ldots \ \tilde{\mathbf{v}}_N^T(t) \ \tilde{\mathbf{b}}_\omega^T(t)]^T \in \mathbb{R}^{3(N+1)}$ and

$$\mathcal{A}_1(t) = -\text{diag}(\alpha_1\mathbf{I} + \mathbf{S}(\boldsymbol{\omega}_m(t)),\ldots,\alpha_N\mathbf{I} + \mathbf{S}(\boldsymbol{\omega}_m(t)),\mathbf{0}) + \begin{bmatrix} \mathbf{0} & \ldots & \mathbf{0} & -\mathbf{S}(\mathbf{v}_1(t)) \\ \vdots & & \vdots & \vdots \\ \mathbf{0} & \ldots & \mathbf{0} & -\mathbf{S}(\mathbf{v}_N(t)) \\ -\beta_1\mathbf{S}(\mathbf{v}_1(t)) & \ldots & -\beta_N\mathbf{S}(\mathbf{v}_N(t)) & \mathbf{0} \end{bmatrix}.$$

Before presenting the main result of this section, the following lemma is introduced.

Lemma 1. *Let $\mathbf{f}(t) : [t_0,t_f] \subset \mathbb{R} \to \mathbb{R}^n$ be a continuous and two times continuously differentiable function on $\mathcal{I} := [t_0,t_f]$, $T := t_f - t_0 > 0$, and such that $\mathbf{f}(t_0) = \mathbf{0}$. Further assume that*

$$\max_{t\in\mathcal{I}} \|\ddot{\mathbf{f}}(t)\| \leq C.$$

If

$$\exists : \|\dot{\mathbf{f}}(t^*)\| \geq \alpha^*, \quad \alpha^* > 0, \quad t^* \in \mathcal{I}$$

then

$$\exists : \|\mathbf{f}(t_0+\delta^*)\| \geq \beta^*. \quad 0<\delta^*\leq T \quad \beta^*>0$$

Proof. This is a particular case of Batista, Silvestre, and Oliveira (2011, Proposition 4.2). □

The following theorem is the main result of this section.

Theorem 1. *Under Assumption 1, consider the bias observer (4), where $\alpha_i>0$, $\beta_i>0$, $i=1,\ldots,N$, are positive scalar parameters. Then, the origin of the observer error dynamics (5) is a globally exponentially stable equilibrium point.*

Proof. Consider the Lyapunov function candidate

$$V_1(t) := \tilde{\mathbf{x}}_1^T(t)\mathbf{D}\tilde{\mathbf{x}}_1(t) = \frac{1}{2}\sum_{i=1}^{N}\beta_i\|\tilde{\mathbf{v}}_i(t)\|^2+\frac{1}{2}\|\tilde{\mathbf{b}}_\omega(t)\|^2,$$

where $\mathbf{D}$ is the block diagonal matrix

$$\mathbf{D} := \tfrac{1}{2}\mathrm{diag}(\beta_1\mathbf{I},\ldots,\beta_N\mathbf{I},\mathbf{I}).$$

Clearly,

$$\gamma_1\|\tilde{\mathbf{x}}_1(t)\|^2 \leq V_1(t) \leq \gamma_2\|\tilde{\mathbf{x}}_1(t)\|^2, \tag{6}$$

where

$$\gamma_1 := \tfrac{1}{2}\min(1,\beta_1,\ldots,\beta_N)$$

and

$$\gamma_2 := \tfrac{1}{2}\max(1,\beta_1,\ldots,\beta_N).$$

The time derivative of $V_1(t)$ can be written as

$$\dot{V}_1(t) = -\tilde{\mathbf{x}}_1^T(t)\mathbf{C}_1^T\mathbf{C}_1\tilde{\mathbf{x}}_1(t) \leq 0, \tag{7}$$

where

$$\mathbf{C}_1 = \begin{bmatrix} \sqrt{\alpha_1\beta_1} & \mathbf{0} & \ldots & \mathbf{0} & \mathbf{0} \\ \mathbf{0} & \ddots & \ddots & \vdots & \vdots \\ \vdots & \ddots & \ddots & \mathbf{0} & \mathbf{0} \\ \mathbf{0} & \ldots & \mathbf{0} & \sqrt{\alpha_N\beta_N} & \end{bmatrix} \in \mathbb{R}^{3N\times 3(N+1)}.$$

It is well known that, if in addition to (6) and (7), the pair $(\mathcal{A}_1(t),\mathbf{C}_1)$ is uniformly completely observable, then the origin of the linear time-varying system (5) is a globally exponentially stable equilibrium point, see Khalil (2001, Example 8.11). The remainder of the proof amounts to show that the pair $(\mathcal{A}_1(t),\mathbf{C}_1)$ is uniformly completely observable. For any piecewise continuous, bounded matrix $\mathbf{K}_1(t)$, of compatible dimensions, uniform complete observability of the pair $(\mathcal{A}_1(t),\mathbf{C}_1)$ is equivalent to uniform complete observability of the pair $(\mathbf{A}_1(t),\mathbf{C}_1)$, with $\mathbf{A}_1(t) := \mathcal{A}_1(t)-\mathbf{K}_1(t)\mathbf{C}_1$, see Ioannou and Sun (1995, Lemma 4.8.1). Now, notice that, attending to the particular forms of $\mathbf{C}_1$ and $\mathcal{A}_1(t)$, there exists a continuous bounded matrix $\mathbf{K}_1(t)$, which depends explicitly on the observer parameters, the rate gyro readings, $\boldsymbol{\omega}_m(t)$, and the vector observations $\mathbf{v}_i(t)$, $i=1,\ldots,N$, such that

$$\mathbf{A}_1(t) = \begin{bmatrix} \mathbf{0} & \ldots & \mathbf{0} & -\mathbf{S}(\mathbf{v}_1(t)) \\ \vdots & & \vdots & \vdots \\ \vdots & & \vdots & -\mathbf{S}(\mathbf{v}_N(t)) \\ \mathbf{0} & \ldots & \mathbf{0} & \mathbf{0} \end{bmatrix}.$$

The expression of $\mathbf{K}_1(t)$ is not presented here as it is evident from the context and it is not required in the sequel. It remains to show that the pair $(\mathbf{A}_1(t),\mathbf{C}_1)$ is uniformly completely observable, i.e., that there exist positive constants ε_1, ε_2, and δ such that

$$\varepsilon_1\mathbf{I} \preceq \mathcal{W}(t,t+\delta) \preceq \varepsilon_2\mathbf{I} \tag{8}$$

for all $t\geq t_0$, where $\mathcal{W}(t_0,t_f)$ is the observability Gramian associated with the pair $(\mathbf{A}_1(t),\mathbf{C}_1)$ on $[t_0,t_f]$. Since the entries of both $\mathbf{A}_1(t)$ and $\mathbf{C}_1$ are continuous and bounded, the right side of (8) is evidently verified. Therefore, only the left side of (8) requires verification. Let

$$\mathbf{d} = \begin{bmatrix} \mathbf{d}_1 \\ \vdots \\ \mathbf{d}_{N+1} \end{bmatrix} \in \mathbb{R}^{3(N+1)}, \quad \mathbf{d}_i \in \mathbb{R}^3, \quad i=1,\ldots,N+1$$

be a unit vector and define

$$\mathbf{f}(\tau,t) := \begin{bmatrix} \sqrt{\alpha_1\beta_1}[\mathbf{d}_1-\int_t^\tau \mathbf{S}(\mathbf{v}_1(\sigma))\mathbf{d}_{N+1}d\sigma] \\ \vdots \\ \sqrt{\alpha_N\beta_N}[\mathbf{d}_N-\int_t^\tau \mathbf{S}(\mathbf{v}_N(\sigma))\mathbf{d}_{N+1}d\sigma] \end{bmatrix} \in \mathbb{R}^{3N},$$

$\tau\in[t,t+\delta]$, $t\geq t_0$. It is easy to show that

$$\mathbf{d}^T\mathcal{W}(t,t+\delta)\mathbf{d} = \int_t^{t+\delta}\|\mathbf{f}(\tau,t)\|^2\,d\tau.$$

If there exists i, $1\leq i\leq N$, such that $\mathbf{d}_i\neq\mathbf{0}$, then it is clear that $\|\mathbf{f}(t,t)\|=\lambda_1>0$ for all $t\geq t_0$. On the other hand, if $\mathbf{d}_i=\mathbf{0}$ for all $i=1,\ldots,N$, then it must be $\|\mathbf{d}_{N+1}\|=1$, $\mathbf{f}(t,t)=\mathbf{0}$, and

$$\left.\frac{\partial\mathbf{f}}{\partial\tau}(\tau,t)\right|_{\tau=t} = \begin{bmatrix} -\sqrt{\alpha_1\beta_1}\mathbf{S}(\mathbf{v}_1(t)) \\ \vdots \\ -\sqrt{\alpha_N\beta_N}\mathbf{S}(\mathbf{v}_N(t)) \end{bmatrix}\mathbf{d}_{N+1}$$

for all $t\geq t_0$. Now, notice that, under Assumption 1, and from the definition of the vector observations, there exist i and j such that $\mathbf{v}_i(t)$ and $\mathbf{v}_j(t)$ are non-collinear for all t. Therefore, there exists $\lambda_2>0$ such that

$$\left\|\left.\frac{\partial\mathbf{f}}{\partial\tau}(\tau,t)\right|_{\tau=t}\right\| \geq \lambda_2$$

for all $t\geq t_0$. In addition, the second derivative of $\mathbf{f}$ is bounded as the angular velocity is assumed bounded. Therefore, using Lemma 1, there exists $\delta_1>0$ and $\lambda_3>0$ such that

$$\|\mathbf{f}(t+\delta_1,t)\| \geq \lambda_3$$

for all $t\geq t_0$. Therefore,

$$\underset{\substack{\lambda^*>0\\ \delta^*>0}}{\exists}\ \underset{t\geq t_0}{\forall}\ \underset{\substack{\mathbf{d}\in\mathbb{R}^{3(N+1)}\\ \|\mathbf{d}\|=1}}{\forall} : \|\mathbf{f}(t+\delta^*,t)\| \geq \lambda^*,$$

and, using Lemma 1 again

$$\underset{\substack{\epsilon_1>0\\ \delta>0}}{\exists}\ \underset{t\geq t_0}{\forall}\ \underset{\substack{\mathbf{d}\in\mathbb{R}^{3(N+1)}\\ \|\mathbf{d}\|=1}}{\forall} : \mathbf{d}^T\mathcal{W}(t,t+\delta)\mathbf{d} \geq \varepsilon_1,$$

which completes the conditions for uniformly completely observable and therefore concludes the proof. □

3.2. Attitude observer

This section proposes an attitude observer assuming that the rate gyro bias is known. In addition, the following assumption is considered.

Assumption 2. The matrix $[\mathbf{r}_1 \ldots \mathbf{r}_N] \in \mathbb{R}^{3\times 3N}$ has full rank.

Remark 1. It is important to stress that, given a set of reference vectors (and corresponding vector observations) that satisfy Assumption 1, it is always possible to construct a set of reference vectors (and corresponding vector observations) such that Assumption 2 is satisfied. Indeed, let $\mathbf{r}_i\in\mathbb{R}^3$ and $\mathbf{r}_j\in\mathbb{R}^3$ denote two non-collinear reference vectors. Then, notice that the set of reference vectors $\{\mathbf{r}_1,\ldots,\mathbf{r}_N,\mathbf{r}_i\times\mathbf{r}_j\}$ satisfies Assumption 2, to which corresponds the set of vector observations $\{\mathbf{v}_1(t),\ldots,\mathbf{v}_N(t),\mathbf{v}_i(t)\times\mathbf{v}_j(t)\}$. Therefore, Assumption 2 does not impose, in practice, any conservativeness whatsoever.

In order to simplify the derivation of the attitude observer and the corresponding proofs, consider a column representation of the rotation matrix $\mathbf{R}(t)$ given by

$$\boldsymbol{x}_2(t) = \begin{bmatrix} \mathbf{z}_1(t) \\ \mathbf{z}_2(t) \\ \mathbf{z}_3(t) \end{bmatrix} \in \mathbb{R}^9,$$

where

$$\mathbf{R}(t) = \begin{bmatrix} \mathbf{z}_1^T(t) \\ \mathbf{z}_2^T(t) \\ \mathbf{z}_3^T(t) \end{bmatrix}, \quad \mathbf{z}_i(t) \in \mathbb{R}^3, \quad i = 1, \ldots, 3.$$

It is straightforward to show that

$$\dot{\boldsymbol{x}}_2(t) = -\mathbf{S}_3(\boldsymbol{\omega}_m(t) - \mathbf{b}_\omega(t))\boldsymbol{x}_2(t),$$

where

$$\mathbf{S}_3(\mathbf{x}) := \operatorname{diag}(\mathbf{S}(\mathbf{x}), \mathbf{S}(\mathbf{x}), \mathbf{S}(\mathbf{x})) \in \mathbb{R}^{9\times 9}, \quad \mathbf{x} \in \mathbb{R}^3.$$

From (2) it is possible to write the vector observations as a function of the column representation of the rotation matrix, as given by

$$\mathbf{v}(t) = \mathbf{C}_2\boldsymbol{x}_2(t),$$

where

$$\mathbf{v}(t) = \begin{bmatrix} \mathbf{v}_1(t) \\ \vdots \\ \mathbf{v}_N(t) \end{bmatrix} \in \mathbb{R}^{3N}$$

and

$$\mathbf{C}_2 = \begin{bmatrix} r_{11} & 0 & 0 & r_{12} & 0 & 0 & r_{13} & 0 & 0 \\ 0 & r_{11} & 0 & 0 & r_{12} & 0 & 0 & r_{13} & 0 \\ 0 & 0 & r_{11} & 0 & 0 & r_{12} & 0 & 0 & r_{13} \\ & & & & \vdots & & & & \\ r_{N1} & 0 & 0 & r_{N2} & 0 & 0 & r_{N3} & 0 & 0 \\ 0 & r_{N1} & 0 & 0 & r_{N2} & 0 & 0 & r_{N3} & 0 \\ 0 & 0 & r_{N1} & 0 & 0 & r_{N2} & 0 & 0 & r_{N3} \end{bmatrix},$$

$\mathbf{C}_2 \in \mathbb{R}^{3N\times 9}$, where

$$\mathbf{r}_i = \begin{bmatrix} r_{i1} \\ r_{i2} \\ r_{i3} \end{bmatrix} \in \mathbb{R}^3.$$

Notice that, under Assumption 2, matrix $\mathbf{C}_2$ has full rank.

Consider the attitude observer given by

$$\dot{\hat{\boldsymbol{x}}}_2(t) = -\mathbf{S}_3(\boldsymbol{\omega}_m(t) - \mathbf{b}_\omega(t))\hat{\boldsymbol{x}}_2(t) + \mathbf{C}_2^T\mathbf{Q}^{-1}[\mathbf{v}(t) - \mathbf{C}_2\hat{\boldsymbol{x}}_2(t)], \tag{9}$$

where $\mathbf{Q} = \mathbf{Q}^T \in \mathbb{R}^{3N\times 3N}$ is a positive definite matrix, and define the error variable $\tilde{\boldsymbol{x}}_2(t) = \boldsymbol{x}_2(t) - \hat{\boldsymbol{x}}_2(t)$. Then, the observer error dynamics are given by

$$\dot{\tilde{\boldsymbol{x}}}_2(t) = \mathcal{A}_2(t)\tilde{\boldsymbol{x}}_2(t), \tag{10}$$

where

$$\mathcal{A}_2(t) := -[\mathbf{S}_3(\boldsymbol{\omega}_m(t) - \mathbf{b}_\omega(t)) + \mathbf{C}_2^T\mathbf{Q}^{-1}\mathbf{C}_2].$$

The following theorem is the main result of this section.

Theorem 2. *Suppose that the rate gyro bias is known and consider the attitude observer* (9), *where* $\mathbf{Q} \succ \mathbf{0}$ *is a design parameter. Then, under Assumption 2, the origin of the observer error dynamics* (10) *is a globally exponentially stable equilibrium point.*

Proof. Consider the Lyapunov candidate function

$$V_2(t) := \tfrac{1}{2}\|\tilde{\boldsymbol{x}}_2(t)\|^2.$$

It is straightforward to show that

$$\dot{V}_2(t) = -\tilde{\boldsymbol{x}}_2^T(t)\mathbf{C}_2^T\mathbf{Q}^{-1}\mathbf{C}_2\tilde{\boldsymbol{x}}_2(t).$$

Now, as $\mathbf{C}_2$ is a constant matrix with full rank and $\mathbf{Q}$ is a positive definite matrix, it follows that $\mathbf{C}_2^T\mathbf{Q}^{-1}\mathbf{C}_2 \succ \mathbf{0}$. Therefore,

$$\dot{V}_2(t) \le -\lambda_{min}(\mathbf{C}_2^T\mathbf{Q}^{-1}\mathbf{C}_2)\|\tilde{\boldsymbol{x}}_2(t)\|^2,$$

where $\lambda_{min}(\mathbf{X})$ corresponds to the minimum eigenvalue of matrix $\mathbf{X}$. This concludes the proof, see Khalil (2001, Theorem 4.10). □

3.3. Cascade observer

This section presents the overall cascade observer and its stability analysis. In Section 3.1 an observer was derived, based directly on the vector observations, that provides an estimate of the bias, with globally exponentially stable error dynamics. The idea of the cascade observer is to feed the attitude observer proposed in Section 3.2 with the bias estimate provided by the bias observer proposed in Section 3.1. The final nonlinear cascade observer reads as

$$\begin{cases} \dot{\hat{\mathbf{v}}}_1(t) = -\mathbf{S}(\boldsymbol{\omega}_m(t))\hat{\mathbf{v}}_1(t) - \mathbf{S}(\mathbf{v}_1(t))\hat{\mathbf{b}}_\omega(t) + \alpha_1\tilde{\mathbf{v}}_1(t), \\ \vdots \\ \dot{\hat{\mathbf{v}}}_N(t) = -\mathbf{S}(\boldsymbol{\omega}_m(t))\hat{\mathbf{v}}_N(t) - \mathbf{S}(\mathbf{v}_N(t))\hat{\mathbf{b}}_\omega(t) + \alpha_N\tilde{\mathbf{v}}_N(t), \\ \dot{\hat{\mathbf{b}}}_\omega(t) = \sum_{i=1}^N \beta_i\mathbf{S}(\mathbf{v}_i(t))\tilde{\mathbf{v}}_i(t), \\ \dot{\hat{\boldsymbol{x}}}_2(t) = -\mathbf{S}_3(\boldsymbol{\omega}_m(t) - \hat{\mathbf{b}}_\omega(t))\hat{\boldsymbol{x}}_2(t) + \mathbf{C}_2^T\mathbf{Q}^{-1}[\mathbf{v}(t) - \mathbf{C}_2\hat{\boldsymbol{x}}_2(t)]. \end{cases} \tag{11}$$

The error dynamics corresponding to the bias observer are the same and therefore Theorem 1 applies. Evidently, the use of an estimate of the bias instead of the bias itself in the attitude observer introduces an error, and the stability of the system must be further examined. In this situation, the error dynamics of the cascade observer can be written as

$$\begin{cases} \dot{\tilde{\boldsymbol{x}}}_1(t) = \mathcal{A}_1(t)\tilde{\boldsymbol{x}}_1(t), \\ \dot{\tilde{\boldsymbol{x}}}_2(t) = [\mathcal{A}_2(t) - \mathbf{S}_3(\tilde{\mathbf{b}}_\omega(t))]\tilde{\boldsymbol{x}}_2(t) + \mathbf{u}_2(t), \end{cases} \tag{12}$$

where

$$\mathbf{u}_2(t) := \mathbf{S}_3(\tilde{\mathbf{b}}_\omega(t))\boldsymbol{x}_2(t).$$

The following theorem is the main result of the paper.

Theorem 3. *Consider the cascade attitude observer* (11). *Then, in the conditions of Theorems 1 and 2, the origin of the observer error dynamics* (12) *is a globally exponentially stable equilibrium point.*

Proof. That $\tilde{\boldsymbol{x}}_1 = \mathbf{0}$ is a globally exponentially stable equilibrium point follows directly from Theorem 1. Next, it is shown that $\tilde{\boldsymbol{x}}_2 = \mathbf{0}$ is a globally exponentially stable equilibrium point of (12). First, consider the perturbed system

$$\dot{\tilde{\boldsymbol{x}}}_2(t) = [\boldsymbol{\mathcal{A}}_2(t) - \mathbf{S}_3(\tilde{\mathbf{b}}_\omega(t))]\tilde{\boldsymbol{x}}_2(t). \tag{13}$$

From Theorem 1 it follows that

$$\lim_{t\to 0}\|\mathbf{S}_3(\tilde{\mathbf{b}}_\omega(t))\| = 0.$$

Moreover, from Theorem 2, the origin of the undisturbed system

$$\dot{\tilde{\boldsymbol{x}}}_2(t) = \mathcal{A}_2(t)\tilde{\boldsymbol{x}}_2(t)$$

is a globally exponentially stable equilibrium point. Therefore, it is possible to conclude that the origin of the perturbed system (13) is a globally exponentially stable equilibrium point, see Khalil (2001, Example 9.6). Now, notice that, since $\mathbf{x}_2(t)$ corresponds to a column representation of the rotation matrix, which is norm-bounded, and $\tilde{\mathbf{b}}_\omega(t)$ converges globally exponentially fast to zero, it follows that $\mathbf{u}_2(t)$ converges globally exponentially fast to zero. Therefore, the dynamics of $\tilde{\boldsymbol{x}}_2(t)$ correspond to those of a GES linear system driven by an exponentially decaying disturbance, from which follows that $\tilde{\mathbf{x}}_2 = \mathbf{0}$ is a globally exponentially stable equilibrium point, therefore concluding the proof. □

3.4. Solution refinements

3.4.1. Full cascade observer

In the cascade observer proposed in Section 3.3, the attitude observer considers only the bias estimate provided by the bias observer and the vector estimates are disregarded. Indeed, the observer employs, for feedback purposes, the output $\mathbf{v}(t)$ instead of the estimate $\hat{\mathbf{v}}(t)$. For performance purposes, particularly in the presence of sensor noise, it may be better to employ the vector estimate $\hat{\mathbf{v}}(t)$ provided by the bias observer. It should be stressed that the nominal asymptotic stability analysis is not affected. Indeed, for the full cascade observer

$$\begin{cases} \dot{\hat{\mathbf{v}}}_1(t) = -\mathbf{S}(\boldsymbol{\omega}_m(t))\hat{\mathbf{v}}_1(t) - \mathbf{S}(\mathbf{v}_1(t))\hat{\mathbf{b}}_\omega(t) + \alpha_1\tilde{\mathbf{v}}_1(t), \\ \vdots \\ \dot{\hat{\mathbf{v}}}_N(t) = -\mathbf{S}(\boldsymbol{\omega}_m(t))\hat{\mathbf{v}}_N(t) - \mathbf{S}(\mathbf{v}_N(t))\hat{\mathbf{b}}_\omega(t) + \alpha_N\tilde{\mathbf{v}}_N(t), \\ \dot{\hat{\mathbf{b}}}_\omega(t) = \sum_{i=1}^{N} \beta_i \mathbf{S}(\mathbf{v}_i(t))\tilde{\mathbf{v}}_i(t), \\ \dot{\hat{\mathbf{x}}}_2(t) = -\mathbf{S}_3(\boldsymbol{\omega}_m(t) - \hat{\mathbf{b}}_\omega(t))\hat{\mathbf{x}}_2(t) + \mathbf{C}_2^T\mathbf{Q}^{-1}[\hat{\mathbf{v}}(t) - \mathbf{C}_2\hat{\mathbf{x}}_2(t)], \end{cases}$$

the error dynamics are similar to (12), but with

$$\mathbf{u}_2(t) = \mathbf{S}_3(\tilde{\mathbf{b}}_\omega(t))\mathbf{x}_2(t) + \mathbf{C}_2^T\mathbf{Q}^{-1}\tilde{\mathbf{v}}(t).$$

Evidently, the steps of Theorem 3 apply yielding the same properties, as the additional term $\mathbf{C}_2^T\mathbf{Q}^{-1}\tilde{\mathbf{v}}(t)$ converges globally exponentially fast to zero.

3.4.2. Orthogonalization step

The cascade observer proposed in the paper yields an estimate of the rotation matrix $\mathbf{R}(t)$ given by

$$\hat{\mathbf{R}}(t) = \begin{bmatrix} \hat{\mathbf{z}}_1^T(t) \\ \hat{\mathbf{z}}_2^T(t) \\ \hat{\mathbf{z}}_3^T(t) \end{bmatrix}, \quad \hat{\mathbf{z}}_i(t) \in \mathbb{R}^3, \quad i = 1, \ldots, 3,$$

where

$$\hat{\mathbf{x}}_2(t) = \begin{bmatrix} \hat{\mathbf{z}}_1(t) \\ \hat{\mathbf{z}}_2(t) \\ \hat{\mathbf{z}}_3(t) \end{bmatrix} \in \mathbb{R}^9.$$

However, the estimate of the rotation matrix, $\hat{\mathbf{R}}(t)$, is not necessarily a rotation matrix as there is nothing in the observer structure imposing the restriction $\hat{\mathbf{R}}(t) \in SO(3)$. In fact, if this restriction is imposed, it is actually impossible to achieve global asymptotic stabilization due to topological limitations, see Bhat and Bernstein (2000). Nevertheless, the estimation error of the proposed observer converges globally exponentially fast to zero and therefore the corresponding rotation matrix restrictions are verified asymptotically.

In practice, both the vector observations and the rate gyro readings are subject to noise, which induces errors in the rotation matrix estimate not related to the initial transients that appear due to possible mismatch of initial conditions. In these conditions, the error converges to a tight neighborhood of zero and estimates arbitrarily close to $SO(3)$ can be obtained by employing computationally efficient orthogonalization cycles, as given by

$$\hat{\mathbf{R}}_f(t) = \tfrac{1}{2}(\hat{\mathbf{R}}(t) + [\hat{\mathbf{R}}^T(t)]^{-1}),$$

see Bar-Itzhack and Meyer (1976). Experimental results reveal that with two cycles the orthogonality error is of the same magnitude of the computational accuracy of low-cost hardware (below 10^{-12}). The projection of the estimate on $SO(3)$ is an alternative to the orthogonalization cycles. Although more expensive, it does provide solutions explicitly on $SO(3)$.

During the initial transients, which typically last less than 10 s, it may happen that the previous solution is not well-defined. In this case, the attitude may be simply obtained from the solution of the Wahba's problem as in traditional solutions resorting directly to the vector observations.

4. Simulation results

In order to evaluate the performance of the proposed observer, simulations were carried out and two examples are shown in this section, without and with sensor noise.

In the simulations the initial attitude was set to $\mathbf{R}(0) = \mathbf{I}$, while the evolution of the angular velocity is depicted in Fig. 1. The rate gyro bias was chosen as $\mathbf{b}_\omega(t) = [-0.2\ 0.4\ 0.6]^T$ (°/s). Finally, magnetic and gravitational field readings are assumed to be available as vector observations, which correspond, in general, to non-collinear inertial vectors, and therefore Theorem 3 applies. The third vector observation results from the cross product between the acceleration of gravity and the magnetic field. The bias observer parameters were chosen as $\alpha_1 = (9.8/0.008)10^{-3}$, $\alpha_2 = (0.5/0.0015)10^{-3}$, and $\beta_1 = \beta_2 = 10^{-3}$, which are related to the norm of the vector observations and the noise of the sensors, which is present in the second simulation only. The attitude observer parameter was chosen as $\mathbf{Q} = 0.25\mathbf{I}$ and all the initial estimates of the bias observer were set to zero, for convergence illustration purposes, while the initial rotation estimate is $\hat{\mathbf{R}}(0) = \text{diag}(-1, -1, 1)$.

The evolution of the Lyapunov functions $V_1(t)$ and $V_2(t)$ is depicted in Fig. 2, where a logarithmic scale is employed on the y-axis. Clearly, the error converges exponentially fast to zero, as expected. In order to evaluate the orthogonality of the proposed solution, the evolution of the orthogonality error, expressed as $\|\hat{\mathbf{R}}(t)\hat{\mathbf{R}}^T(t) - \mathbf{I}\|$, is depicted in Fig. 3, where a logarithmic scale is

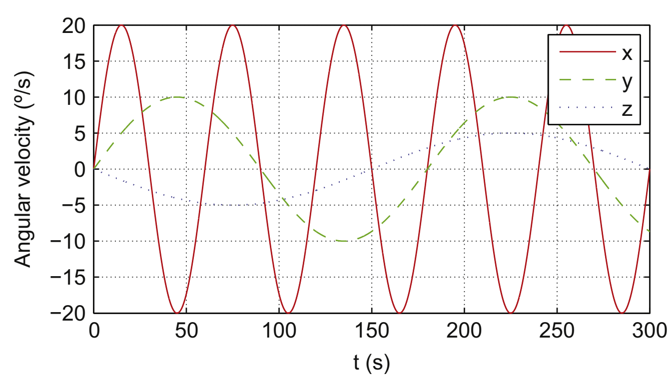

Fig. 1. Evolution of the angular velocity $\boldsymbol{\omega}(t)$.

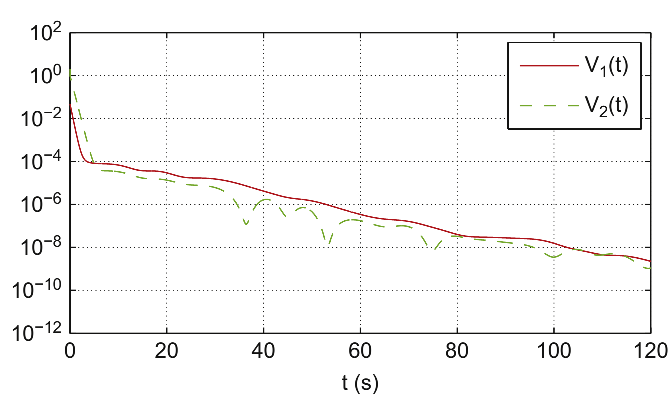

Fig. 2. Evolution of the Lyapunov functions $V_1(t)$ and $V_2(t)$.

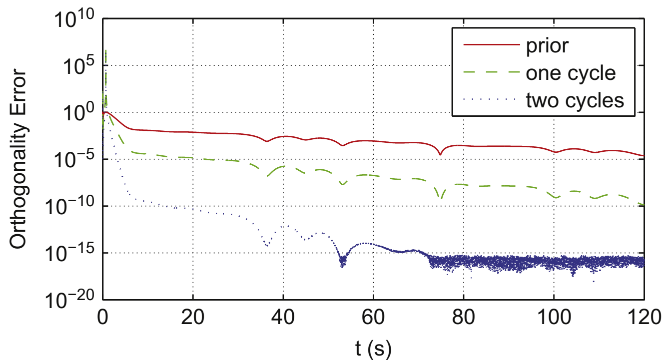

Fig. 3. Evolution of the orthogonality error $\|\hat{\mathbf{R}}(t)\hat{\mathbf{R}}^T(t)-\mathbf{I}\|$.

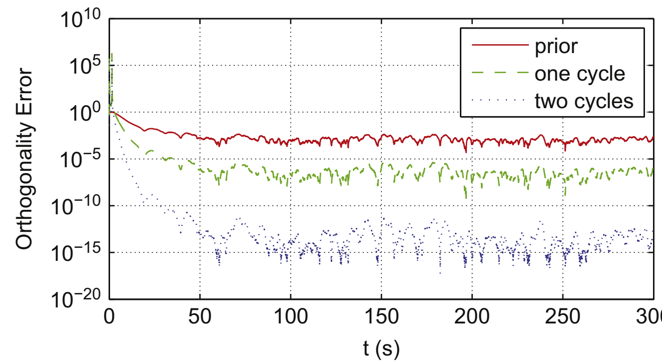

Fig. 5. Evolution of the orthogonality error $\|\hat{\mathbf{R}}(t)\hat{\mathbf{R}}^T(t)-\mathbf{I}\|$.

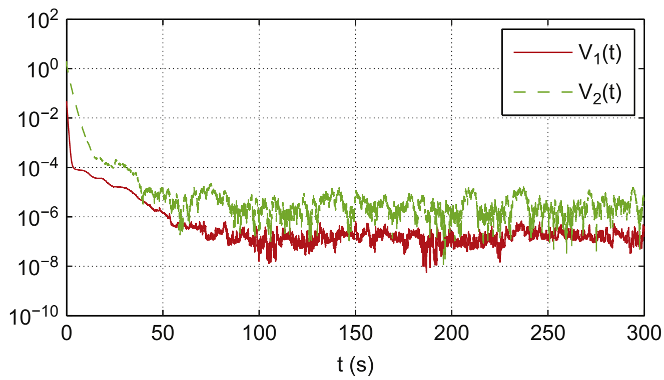

Fig. 4. Evolution of the Lyapunov functions $V_1(t)$ and $V_2(t)$.

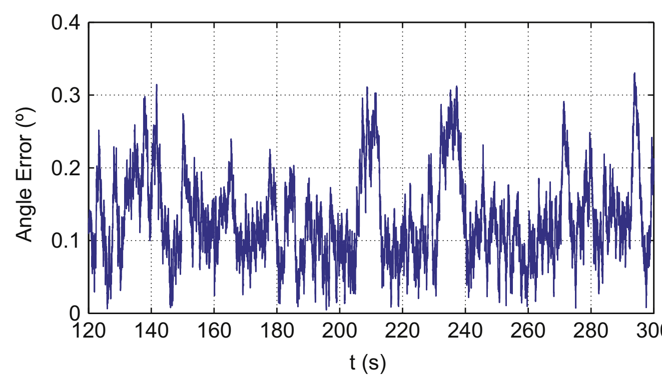

Fig. 6. Evolution of the angle error $\tilde{\theta}(t)$.

also employed on the y-axis. The error prior to the orthogonalization process converges to zero, as expected. The introduction of a single orthogonalization cycle, which is computationally efficient, further reduces the level of the orthogonalization error, while with two orthogonalization steps the error quickly converges to values that are close to the numerical accuracy of the present simulation, which is evident by the final shattering around 10^{-16}. Notice that there is an initial spike in the orthogonalization error after the orthogonalization cycles. This is due to the initial transients and the fact that the orthogonality of the corresponding rotation matrix estimate is not explicitly enforced. In fact, if this had been enforced, there would be topological limitations for achieving global asymptotic stability, see Bhat and Bernstein (2000). Nevertheless, the error converges exponentially fast to zero and the orthogonality property is verified asymptotically.

In order to evaluate the performance of the proposed solutions in a realistic simulation environment, the previous simulation was modified and sensor noise was considered on the angular velocity readings and the body-fixed vector observations. In particular, additive, zero-mean, white Gaussian noise was considered, with standard deviations of 0.95°/s for the angular velocity, 0.008 m/s^2 for the gravity acceleration, and 0.0015 Gauss for the magnetic field measurements, in accordance with the chosen observer gains. Notice that the specifications of the noise correspond to a very low-grade sensor suite. The observer parameters and initial conditions are the same of the previous simulation but a longer simulation was carried out, in time, to better evaluate the steady-state performance of the proposed solution. The evolution of the Lyapunov functions is depicted in Fig. 4, where a logarithmic scale is employed on the y-axis. The effect of the noise is now visible but in steady-state the error stays close to 10^{-5}. The evolution of the orthogonality error is shown in Fig. 5. Again, the initial large error after the orthogonalization steps appears due to the fact that, during the initial transients, the rotation estimate passes close to singularity.

Nevertheless, the observer quickly enters the steady-state zone, and the effect of the orthogonalization steps is visible, which translates in orthogonality errors below 10^{-6} in steady-state with just one orthogonalization step and well below 10^{-12} with two orthogonalization steps. In order to evaluate the overall attitude performance, and for the purpose of performance evaluation only, an additional error variable is defined as $\tilde{\mathbf{R}}(t)= \mathbf{R}^T(t)\hat{\mathbf{R}}(t)$, which corresponds to the rotation matrix error. Using the Euler angle–axis representation for this new error variable,

$$\tilde{\mathbf{R}}(t)=\mathbf{I}\cos(\tilde{\theta}(t))+[1-\cos(\tilde{\theta}(t))]\tilde{\mathbf{d}}(t)\tilde{\mathbf{d}}^T(t)-\mathbf{S}(\tilde{\mathbf{d}}(t))\sin(\tilde{\theta}(t)), \tag{14}$$

where $0\le\tilde{\theta}(t)\le\pi$ and $\tilde{\mathbf{d}}(t)\in\mathbb{R}^3, \|\tilde{\mathbf{d}}(t)\|=1$, are the angle and axis that represent the rotation error, the performance of the filter is easily identified from the evolution of $\tilde{\theta}$, which is depicted, after the initial transients fade out, in Fig. 6. As it is possible to see, the angle error remains confined to a tight interval, in spite of the low-grade specifications of the sensors. The mean error is 0.12°.

5. Experimental results

In order to evaluate the proposed solutions in real world applications, the proposed algorithm was tested with the experimental setup described in Batista, Silvestre, Oliveira, and Cardeira (2010), where a high precision Motion Rate Table, Model 2103HT from Ideal Aerosmith (2006), allows for accurate and reliable motion control and yields ground truth data for performance evaluation purposes. The table outputs, in a fixed-frequency profile mode, the angular position of the table with a resolution of 0.00025°. The IMU that was employed is the nanoIMU NA02-0150F50 (MEMSENSE, 2009), from MEMSENSE, which outputs data at a rate of 150 Hz. This 9 degree-of-freedom (DOF) Micro-Electro-Mechanical System (MEMS) device is a miniature, light weight, 3-D digital output sensor (it outputs 3-D acceleration, 3-D angular rate, and 3-D magnetic field data) featuring

RS422 or I2C protocols, with built-in bias, sensitivity, and temperature compensation. The standard deviations of the noise of the outputs of the IMU are the same as those considered in Section 4. Fig. 7 displays the experimental setup mounted on the table top. Unfortunately, the calibration table distorts the magnetic field in the neighborhood of the IMU, even though it was attempted to place the IMU as far as possible from the other components of the experimental setup, by means of a small nonmagnetic bar, which elevates the sensor from the table top. Therefore, magnetic field measurements were simulated in the loop. Sensor noise was naturally added so that the results are as realistic as possible.

The motion rate table has three rotational joints which allow for movement about three orthogonally mounted axes, so-called inner, middle, and outer axis, and that were defined as the x, y, and z axes of the body-fixed reference frame, so that the rotation from body-fixed coordinates to inertial coordinates is given by

$$\mathbf{R}(t)=\mathbf{R}_z(\theta_{out}(t))\mathbf{R}_y(\theta_{mid}(t))\mathbf{R}_x(\theta_{inn}(t)),$$

where $\mathbf{R}_x(.)$, $\mathbf{R}_y(.)$, and $\mathbf{R}_z(.)$ are the rotation matrices about the x, y, and z axes, respectively, and θ_{inn}, θ_{mid}, and θ_{out} are the inner, middle, and outer axis angles, respectively. The evolution of the inner, middle, and outer angles is depicted in Fig. 8. Notice that the angular motion full range is used and if Euler angles were employed problems would have appeared due to singularities. Also, note that the angular velocity $\boldsymbol{\omega}(t)$, which is shown in Fig. 9, reaches interesting values, typical of many autonomous vehicles such as Autonomous Underwater Vehicles, Autonomous Ground Vehicles or Unmanned Air Vehicles.

Fig. 7. Experimental setup.

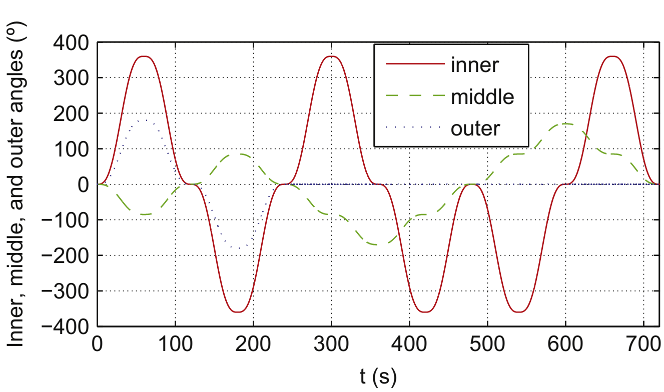

Fig. 8. Evolution of the inner, middle, and outer angles.

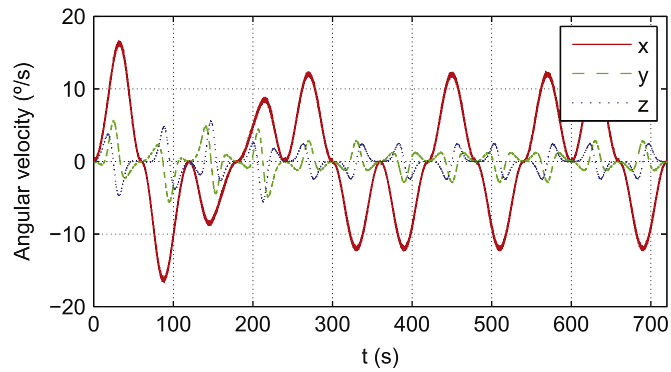

Fig. 9. Evolution of the angular velocity $\boldsymbol{\omega}(t)$.

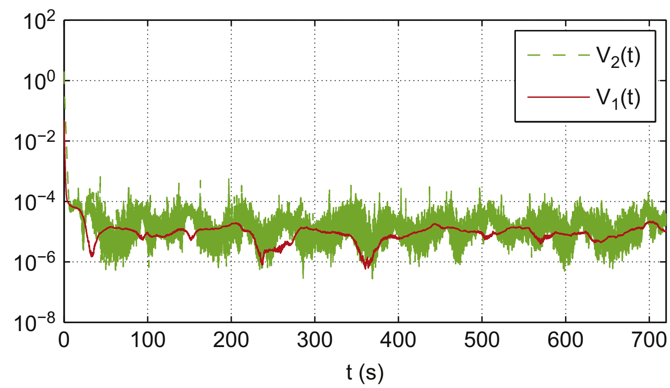

Fig. 10. Evolution of the Lyapunov functions $V_1(t)$ and $V_2(t)$.

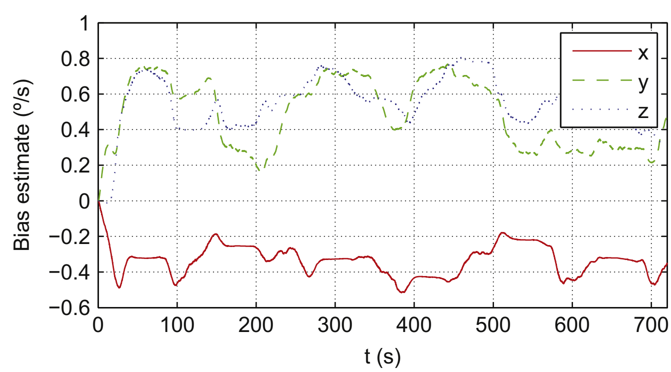

Fig. 11. Evolution of the rate gyro bias estimate.

The observer parameters, as well as the initial estimates, are the same as those presented in Section 4. The evolution of the Lyapunov functions is depicted in Fig. 10. As the true bias is unavailable, in order to compute $V_1(t)$, the true bias was assumed to be identical to the bias estimate provided by an offline bias estimation algorithm, which considers the platform at rest and takes the mean value as the rate gyro bias. As it is possible to see, the convergence rate of the observer is very fast and the steady-state is achieved in less than 10 s. The mean angle error, in terms of the angle–axis parameterization (14), is 0.18°, which is a very good value considering the low-grade specifications of the IMU at hand. It is also comparable with the results obtained in simulation and it compares to a mean error of 0.13° for the solution proposed in Batista et al. (2010). However, the present solution is computationally efficient. Indeed, it does not require the online solution of Riccati equations nor the Wahba's problem, while the solution proposed in Batista et al. (2010) requires all of these. The evolution of the rate gyro bias estimate is shown in Fig. 11. Again, it is possible to conclude that the estimate of the bias quickly converges to steady-state values, with small fluctuations over time, which is quite typical of low-cost units such as the one employed in this experiment.

6. Conclusions

This paper presented the design, analysis, and performance evaluation of a novel cascade observer for attitude estimation. The proposed solution resorts directly to a set of vector observations, in body-fixed coordinates, of known constant reference vectors in inertial coordinates, in addition to rate gyro readings. First, a bias observer is proposed, with globally exponentially stable error (GES) dynamics. Afterwards, an attitude observer, built under the assumption of known rate gyro bias, is proposed, also with GES error dynamics. The final cascade observer results from feeding the attitude observer with the rate gyro bias estimate obtained from the first observer and the error dynamics of the overall cascade system are GES. In addition, an estimate of the rotation matrix is directly obtained, without the explicit solution of the Wahba's problem, and the observer gains do not require the solution of any differential equation. Therefore, the proposed system is computationally efficient and appropriate for application in platforms where computational resources are scarce. Furthermore, the present solution does not exhibit drawbacks common to attitude estimation solutions such as singularities, unwinding phenomena or topological limitations for achieving global asymptotic stability. Simulation results are included that illustrate the achievable performance in the presence of realistic measurements and, finally, very encouraging experimental results are provided resorting to a low-cost, low-power Inertial Measurement Unit. For performance evaluation purposes a Motion Rate Table was employed that provides ground truth data, which allowed to effectively evaluate the proposed solution in absolute terms. Future work includes the comparison of the achieved performance with existing solutions in the literature and commercially available Attitude and Heading Reference Systems.

Acknowledgments

The authors gratefully acknowledge the expertise and contributions of Bruno Cardeira, Luís Sebastião, André Oliveira, and José Tojeira in the development of the experimental setup.

References

Bar-Itzhack, I., & Meyer, J. (1976). On the convergence of iterative orthogonalization processes. *IEEE Transactions on Aerospace and Electronic Systems*, *12*(2), 146–151.

Bar-Itzhack, I., & Oshman, Y. (1985). Attitude determination from vector observations: Quaternion estimation. *IEEE Transactions on Aerospace and Electronic Systems*, *321*(1), 128–136.

Batista, P., Silvestre, C., & Oliveira, P. (2009). Sensor-based complementary globally asymptotically stable filters for attitude estimation. In *Proceedings of the 48th IEEE conference on decision and control*, (pp. 7563–7568). Shanghai, China, December.

Batista, P., Silvestre, C., & Oliveira, P. (2011). On the observability of linear motion quantities in navigation systems. *Systems & Control Letters*, *60*(2), 101–110.

Batista, P., Silvestre, C., Oliveira, P., & Cardeira, B. (2010). Low-cost attitude and heading reference system: Filter design and experimental evaluation. In *Proceedings of the 2010 IEEE international conference on robotics and automation*, (pp. 2624–2629). Anchorage, USA, May.

Bhat, S., & Bernstein, D. (2000). A topological obstruction to continuous global stabilization of rotational motion and the unwinding phenomenon. *Systems & Control Letters*, *39*(1), 63–70.

Campolo, D., Keller, F., & Guglielmelli, E. (2006). Inertial/magnetic sensors based orientation tracking on the group of rigid body rotations with application to wearable devices. In *Proceedings of the 2006 IEEE/RSJ international conference on intelligent robots and systems—IROS 2006* (pp. 4762–4767). Beijing, China.

Chaturvedi, N., Sanyal, A., & McClamroch, N. (2011). Rigid-body attitude control. *IEEE Control Systems Magazine*, *31*(3), 30–51.

Choukroun, D. (2009). Novel results on quaternion modeling and estimation from vector observations. In *Proceedings of the AIAA guidance navigation and control conference*, Chicago, IL, USA, August.

Crassidis, J., Markley, F., & Cheng, Y. (2007). Survey of nonlinear attitude estimation methods. *Journal of Guidance, Control and Dynamics*, *30*(1), 12–28.

Farrell, J. (1970). Attitude determination by Kalman filter. *Automatica*, *6*(5), 419–430.

Ideal Aerosmith, Inc. (2006). *2103HT multi-axis table data sheet*, Rev C. 〈http://www.ideal-aerosmith.com/〉.

Ioannou, P., & Sun, J. (1995). *Robust adaptive control*. Prentice Hall.

Khalil, H. (2001). *Nonlinear systems* (3rd ed.). Prentice Hall.

Mahony, R., Hamel, T., & Pflimlin, J.-M. (2008). Nonlinear complementary filters on the special orthogonal group. *IEEE Transactions on Automatic Control*, *53*(5), 1203–1218.

Martin, P., & Salaun, E. (2010). Design and implementation of a low-cost observer-based attitude and heading reference system. *Control Engineering Practice*, *17*(7), 712–722.

MEMSENSE (2009). *NANO IMU product specification user's guide*, document number PSD-0822, Rev. A. 〈http://www.memsense.com〉.

Metni, N., Pflimlin, J.-M., Hamel, T., & Soueres, P. (2006). Attitude and gyro bias estimation for a VTOL UAV. *Control Engineering Practice*, *14*(12), 1511–1520.

Rehbinder, H., & Ghosh, B. (2003). Pose estimation using line-based dynamic vision and inertial sensors. *IEEE Transactions on Automatic Control*, *48*(2), 186–199.

Sabatini, A. (2006). Quaternion-based extended Kalman filter for determining orientation by inertial and magnetic sensing. *IEEE Transactions on Biomedical Engineering*, *53*(7), 1346–1356.

Sanyal, A., Lee, T., Leok, M., & McClamroch, N. (2008). Global optimal attitude estimation using uncertainty ellipsoids. *Systems & Control Letters*, *57*(3), 236–245.

Tayebi, A., McGilvray, S., Roberts, A., & Moallem, M. (2007). Attitude estimation and stabilization of a rigid body using low-cost sensors. In *Proceedings of the 46th IEEE conference on decision and control*, (pp. 6424–6429). New Orleans, USA, December.

Thienel, J., & Sanner, R. (2003). A coupled nonlinear spacecraft attitude controller and observer with an unknown constant gyro bias and gyro noise. *IEEE Transactions on Automatic Control*, *48*(11), 2011–2015.

Vasconcelos, J., Cunha, R., Silvestre, C., & Oliveira, P. (2007). Landmark based nonlinear observer for rigid body attitude and position estimation. In *Proceedings of the 46th IEEE conference on decision and control*, (pp. 1033–1038). New Orleans, LA, USA, December.